Journal of Applied Research and Technology

www.jart.ccadet.unam.mx
Journal of Applied Research and Technology 17 (2019) 44-56

Original

Matrix and reinforcement materials for low-cost building isolators: an overview of results from experimental tests and numerical simulations

Ingrid E. Madera Sierra*, [a], Johannio Marulanda Casas [b], Peter Thomson [b]

[a] *Departamento de Ingeniería Civil e Industrial, Pontificia Universidad Javeriana Cali, Calle 18 #118-200, Santiago de Cali, Colombia*

[b] *Facultad de Ingeniería, Universidad del Valle, Calle 13 #100-00, Santiago de Cali, Colombia*

Received dd mm aaaa; accepted dd mm aaaa
Available online dd mm aaaa

Abstract: During the last years several options to replace the conventional steel-reinforced isolators have been investigated using different materials for the matrix and reinforcement to implement isolation system in buildings. As alternatives to natural rubber, recycled elastomers derived from tires and industrial leftover, scrap tire rubber pads and nanocomposite rubber, have been proposed. Furthermore, with the goal of replacing the inflexible, thick steel plates, a wide variety of fabric reinforcements, such as nylon, carbon, polyester, polyamide, glass and thin flexible steel plates, have been investigated. The manufacturing process and connections between the devices and the structure (bonded, unbonded and partially bonded) have also been studied. This paper presents an overview of the results from investigations where the mechanical properties of prototypes were determined through horizontal shear and vertical compression tests and, in certain cases, through finite element analysis with hyperelastic models. In order to facilitate the visualization and comparison between investigations, the results are tabulated and plotted. The organization and presentation of the results allows to identify important aspects implemented in different experimental programs and analytical models developed for low-cost isolators.

Keywords: elastomeric isolator; low-cost isolator; fiber-reinforced isolator; hyperelastic models

1. INTRODUCTION

Base isolation is a technique where the structure is uncoupled from the ground due to the installation of isolation bearings in the foundation's structure. This reduces the damaging horizontal motion that earthquakes transmit to structures and decreases the economic and human life losses after an earthquake (Kang, Kang, & Moon, 2003). The effectivity of this system has been demonstrated in several applications (Ledezma-Ramirez, Ferguson, & Brennan, 2010) and places such as Kobe and Los Angeles (Gómez, 2008) and through studies in both high and medium rise buildings (Martelli & Forni, 2010; Mkrtycheva, Dzhinchvelashvilia, & Bunov, 2014; Saiful Islam, Rizwan Hussain, Jameel, & Zamin Jumaat, 2012). The most common types of isolation systems use steel-reinforced multilayer elastomeric and sliding bearings, though there are also systems that combine both devices (Buckle, 2000). With an isolation system, the fundamental horizontal period of the structure is increased and as, a consequence, the pseudo-

* Corresponding author.
E-mail address: ingridm@javerianacali.edu.co (Ingrid E. Madera Sierra)
Peer Review under the responsibility of Universidad Nacional Autónoma de México.

acceleration is reduced. Hence, the earthquake-induced forces and energy in the structure are also reduced (Melkumyan 2013; Naeim & Kelly, 1999). This is possible by installing isolators with sufficient vertical and bending stiffnesses and high horizontal flexibility.

The principal limitation for the use of isolation systems is that the devices are generally large, heavy and expensive (Kang et al., 2003). Their high cost is due to their highly labor-intensive manufacturing process (Moon, Kang, Kang, & Kelly, 2002). Their application is justified for large, expensive buildings but is questionable in the case of common construction buildings (Moon, Kang, Kang, Kim, & Kelly, 2003). The production of low-cost seismic isolation systems using a relatively simple manufacturing process could stimulate applications of this type of earthquake-resistant strategy to ordinary housing and commercial low- to medium-rise buildings for both new and existing buildings (Spizzuoco, Calabrese, & Serino, 2014). Reducing the isolators' cost and weight can be met either by reducing the thickness of the reinforcing steel plates or by replacing the steel with a fabric reinforcement (Kelly & Konstantinidis, 2011). Another aspect that can be modified in these devices is the type of connection used between them and the structure that can either be fully (bonded condition) or partially anchored (unbonded condition). The last option results in less weight, lower cost and easier installation of the isolator.

In several investigations, prototypes have been subjected to compression, combined compression and shear tests to guarantee good behavior under seismic loads (Ashkezari, Aghakouchaka, & Kokabib, 2008; Kang et al., 2003). In some cases, with the use of experimental results, analytical models have been updated using the finite element method. Considering that rubber, as few other materials like cartilage, has a nonlinear viscoelastic behavior (Gent, 2012; Vidal-Lesso, Ledesma Orozco, Lesso Arroyo, & Rodríguez Castro, 2011), these models have been adjusted with different hyperplastic functions and used to represent and predict the isolator's behavior as well as several properties under seismic loads. This paper presents an overview of studies on seismic isolators for buildings using different types of materials for both the matrix and the reinforcement, developed through experimental tests programs. Investigations results with finite element analysis, emphasizing in the hyperelastic models used, are also presented. Finally, with the aim to facilitate the visualization and comparison of these studies, the principal characteristics and mechanical properties of the isolators are tabulated and plotted.

2. MATRIX MATERIALS

Gjorgjiev and Garevski (2013) developed a high damping natural rubber compound (HDR) for bearings. The bearings were produced without internal steel plates and with different number of steel plates. The steel plates were coated with an appropriate adhesive. During testing, the bearings exhibited bilinear behavior until moderate shear strain. At higher strains, the rubber bearings behaved in the nonlinear range and were characterized by an increased stiffness. Stiffness, damping and modulus values obtained from experimental tests demonstrated that HDR could be used to manufacture isolators without a lead core, which means less weight and simpler fabrication. Regarding the issue of ensuring low-acceleration responses, it was suggested that HDR could be used as potential practical protection mechanisms for buildings against strong earthquakes because the motion of the building´s superstructure with an isolator is smoother than without an isolator (Kang & Kang, 2009).

Spizzuoco et al. (2014) substituted natural rubber with a recycled low-cost elastomer, and the reinforcing layers were substituted with fiber sheets; the resulting bearings were significantly lighter and less expensive than traditional isolators. The elastomers used were derived from tires or industrial leftovers; those devices were called recycled rubber–fiber reinforced bearings (RR-FRBs). For adhesion between components, the fiber layers were impregnated with a polyurethane binder. The lateral response of the RR-FRBs was non-linear. During cyclic lateral tests, the isolators exhibited shear deformations that could enhance the seismic efficiency of the bearings. All bearings exhibited a rollover type of deformation when subjected to significantly large lateral loads due to the unbounded boundary condition of the specimen. Vertical compression tests demonstrated that RR-FRBs provide an acceptable vertical stiffness. The tested RR-FRB prototypes had a restricted aspect ratio and their configuration was stable up to limited lateral displacements because the effective lateral stiffness decreased significantly (80%) with increasing amplitude of lateral displacement. This underlined the limits of applicability of base isolation with rubber to light-weight structures.

Therefore, the devices were proposed for heavy masonry buildings, where larger aspect ratios could be adopted Spizzuoco et al. (2014).

Mishra, Igarashi, and Matsushima, (2013) developed an isolator using scrap tire rubber pads (STRP) from the tread section of bus or truck tires. The layers were just stacked one on top of another without applying an adhesive. For the reinforcement, each isolator layer contained five layers of steel cords interleaved and bonded between the rubber layers; those cords had several strands in twisted form and inside tire layers generated a similar effect as the steel layers inside elastomeric isolators (Turer & Özden, 2008). The vertical stiffness of the STRP isolator was sufficient to withstand the structural weight load of buildings as well as to prevent the rocking motion of the structure. The ratio between the vertical and horizontal stiffness was greater than 150; thus, according to standards, the STRP isolator can be used as a base isolation device. The shear deformation capacity of the layer-unbonded STRP isolator was approximately 100% after layer separation. Therefore, proper bonding between the layers is necessary. Due to rollover deformation, the efficiency of the isolation system increased as the lateral displacement increased. The damping ratio of the STRP isolator was higher than the damping ratio of the natural rubber bearing; therefore, additional damping enhancement mechanisms could be avoided (Mishra et al., 2013).

Experimental tests results have shown that modifying fiber-reinforced elastomeric isolators (FREIs) by cutting holes in the center portion of the isolators or removing sections from the sides can enhance their lateral response characteristics. One example of this was made in 2003 by Kang et al. (2003) who created holes and hole plus lead plug within the isolators. From test's result of FREI with hole and lead plug, it was found that the hole and lead plug in FREI had little effect on effective stiffness and effective damping, less than 25% and less than 5%, respectively (Kang et al., 2003). Osgooei, Tait, and Konstantinidis (2014) and Van Engelen, Osgooe, Tait, and Konstantinidis (2014) investigated the lateral response of modified rectangular unbounded FREIs (MR-FREIs) through experimental tests and 3D finite element analysis (Osgooei, Van Engelen, Konstantinidis, & Tait, 2015). Introducing modifications resulted in a reduction in the effective lateral stiffness of the isolators and general improvement in the damping characteristics. Also, the results demonstrated that a full rollover occurs at lower lateral displacements compared with that of unmodified isolators. An increase in the peak shear strain values in the elastomer layers was observed, and the vertical stiffness and compression modulus were highly sensitive to interior modifications and to a lesser extent, exterior modifications (Van Engelen et al., 2014).

With the aim to improve the mechanical properties of a polymer matrix for structural applications, it has been proposed nano and micro fillers, as reinforcement materials, with good results in terms of load carrying and energy absorbing capacities (Hallad et al., 2017). Taking account that the isolator´s behavior is directly related with the characteristics of the rubber used, in 2010 Khanlari, Dehghani, Kokabi, and Razzaghi (2010) developed a device based on nanocomposite rubber compound, called fiber-reinforced nanocomposite elastomeric isolator (FRNEI); for that, a NR/organoclay (3 wt%) nanocomposite were made by melt-mixing in an internal mixer and was used a carbon fabric as a reinforcement. The isolators were tested under vertical load and vertical with shear loads applied simultaneously. The results were compared with those obtained for a carbon FREIs. The experimental works demonstrated a high possibility to replace elastomeric compound in isolators with nanocomposite compound and that the FRNEI had a higher vertical stiffness and vertical to horizontal stiffness ratio than that of FREI (53.86% and 20.71%, respectively) (Khanlari, et al., 2010).

Studies about the response of base isolators built with ten years of difference demonstrated an increase of the device stiffness (Casciati & Faravelli, 2012) and reduction of the damping ratio (Russo, Pauletta, & Cortesia, 2013). That is why, deterioration in the adhesive performance and degradation of the elastomeric properties are significant durability issues which must be periodically controlled during the expected lifetime of the structural system (Casciati & Faravelli, 2012; Russo, et al., 2013). On the other hand, tests made on rubber specimens have demonstrated that the stress levels and the shear stiffness considerably increase while decreasing air temperature, especially when air temperature drops below zero. The cyclic mechanical behavior does not change at high air temperatures and the equivalent viscous damping remains constant over the whole temperature range. Rubber crystallization, due to prolonged exposure to air temperatures below zero, increase the force levels transmitted to the structure, during the first loading cycle. Accordingly, this aspect should be considered, because it affects the structure's design, especially in near-fault regions (Cardone, Donatello, Gesualdi, & Nigro, 2011).

3. REINFORCEMENT MATERIALS

As alternative to the conventional steel reinforced isolator (SREI), Konstantinidis and Kelly (2014) proposed steel-reinforced elastomeric bearings (SREBs), where the reinforcing elements, which are normally thick, inflexible steel plates, were replaced by thin flexible reinforcement. SREBs were able to survive extremely large shear strains, comparable to those expected for conventional seismic isolators under seismic loading. Because SREBs, like FREIs, were often installed in an unbonded condition, there was a possibility of slipping along the supports, both under lateral and under pure compressive loading. It was concluded that the SREBs had much less severe bonding requirements and costs than conventional isolators with the potential of mass-production manufacturing and thus, could be implemented in any type of retrofit of vulnerable buildings (Konstantinidis & Kelly, 2014).

In 2008, Ashkezari et al. (2008) and Strauss et al. (2014) designed and manufactured FREIs, which were compared with an SREI. To create the compound, the woven fibers were completely impregnated with an adhesive. The tests showed that the behavior of the FREI was similar to SREI regarding the vertical stiffness and shear characteristics, such as the effective horizontal stiffness and damping (Strauss, et al., 2014). Therefore, the FREIs could be used for seismic isolation of structures with the advantages of being lighter and simpler to manufacture compared with that of SREIs (Hedayati & Shahria, 2014a, 2014b). The primary differences with FREIs previously reported in the literature were that frictional damping was not produced in the carbon reinforcement fibers and were able to sustain extremely large shear strains (225%) in the presence of top and bottom steel end plates. The shape factor of the elastomer layers did not affect the effective shear modulus and the equivalent viscous damping ratio (Ashkezari et al., 2008).

Taking into account that different types of carbon fibers that are available, Russo et al. (2013) investigated two types of fibers: bi-directional (bd) and quadri-directional (qd). The results showed that the qd specimens had a higher average horizontal stiffness and were vertically stiffer and more dissipative under horizontal loads compared with that of bd specimens due to the greater amount of fibers present in the quadri-directional fabrics. Not all the fibers were glued to the rubber, in particular, the interior fibers; hence, these fibers crawled over one another while the isolator was cyclically subjected to shear deformation. This friction dissipates energy, where this dissipation was greater when more fibers were involved. These properties are favorable because they further reduce the acceleration transferred from the isolator to the structure. Moreover, with the application of a horizontal load, the isolators exhibited stable rollover deformation due to their boundary conditions at the contact surfaces where no mechanical or chemical bonding was realized (Russo et al., 2013).

In pursuit of a different type of fiber, Kang and Kang (2009) used nylon as the reinforcing fiber. The characteristics of the isolators made with this fiber were compared with SREI specimens. Under equal vertical loading, the deformation of the nylon FREI was greater than that of the SREI, which indicates that the vertical loading capacity of nylon FREI was lower than that of SREI. This result is due to the fact that the tensional stiffness of nylon is lower than that of steel. However, the damping of nylon FREI was two times greater than that of SREI. Because the tension stiffness of the nylon could be strengthened by using carbon fiber, a comparative investigation of the test results for nylon FREI, carbon FREI and SREI was made. The analyses showed that for nylon-reinforced structures, both the vertical and horizontal stiffnesses decreased, and in the case of carbon reinforcement, the stiffness increased compared with that of SREI (Kang & Kang, 2009).

In 2008, Mordini and Strauss investigated another type of fiber reinforcement. An isolator made of a rubber body with embedded glass fiber layers (GRFB) was used. The bearing behavior was influenced by the vertical loading and the horizontal displacement and its frequency. The obtained damping values correspond to the production specifications of the rubber; this means that the bearing could effectively provide an isolated structure with targeted damping (Mordini & Strauss, 2008). With the purpose of choosing the best reinforcement between carbon fibers and glass fibers, Moon et al. (2002) and Kang et al. (2003) tested isolators using both options. The results showed that vertical stiffness of carbon fiber reinforcement was higher than that of glass fiber reinforcement. Thus, based on the test results, carbon fiber was selected as the reinforcement of FREI (Kang et al., 2003; Saiful Islam et al., 2012).

A non-conventional types of reinforcements, bidirectional carbon-fiber-reinforced plastics mesh, an

engineering plastic sheet and polyamide fiber, were suggested in 2014 by Naghshineh, Akyüz, and Caner, (2014), Ping et al. (2014), Bakhshi, Jafari, and Tabrizi (2014) respectively. The proposed isolators were tested under vertical and horizontal shear loads and compared with conventional isolators (SREI, FREI). In the first proposal, the fiber-mesh-reinforced bearings had a significant reduction of horizontal stiffness compared with SREI at high levels of vertical load and at high levels of shear strain, and for both cases the damping value was similar. Regarding with the manufactured process, the vulcanization of fiber mesh was more effective than vulcanization of steel plate to rubber, because the rubber bonded to the surface of the fiber and also provided a positive connection between the adjacent layers through the openings of the mesh (Naghshineh, et al., 2014). For the second case, was demonstrated that the engineering plastic plate had a high possibility to replace the steel reinforcement on isolators, achieving a kind of high damping isolator (damping 8%). Also, using the devices with unbounded condition was obtained a lower horizontal stiffness and stress demand on rubber material. In terms of cost, this was less than 10% of a SREI (Ping et al., 2014). In the last case, with a flexible reinforcement the damping increased to 20 and 30 % for carbon and polyamide fiber FREI, respectively. However, due to the high elastic modulus of the carbon fiber, this option rather than polyamide fiber provided more reasonable performance for the isolator (Bakhshi et al., 2014).

4. FINITE ELEMENT MODELS

Results on full-scale buildings with isolation system have demonstrated that the non-linear behavior, deformation and stiffness of the isolation system are close to that observed in tests on rubber samples. Likewise, the value of the period of vibration, the damping and floor's accelerations are similar to the design calculations based on the initial stiffness of the isolation system and the actual weight of the building (Melkumyan et al., 2000). This confirms that it is possible to predict the building's behavior from the sample isolator's properties (Ibrahim, 2008).

In 2013, based on the results and the performed tests on HDR, Gjorgjiev et al. created and used a database to develop a polynomial analytical model of a rubber bearing by matching with experimental tests results. The behavior of the rubber bearing was represented through eight parameters plus the polynomial coefficients. Considering the similarity between the analytical and experimental results, the polynomial model could be used to model isolators made with different rubber compounds instead of using a bilinear simplification. Furthermore, the modification factors of the system properties regarding the effects of aging, temperature and scragging could be included in this model by changing the polynomial coefficients (Gjorgjiev & Garevski, 2013).

In the case of the RR-FRB test representation, a Neo-Hooke finite element analysis (FEA) was used. Because the assumptions on the material behavior, a clear understanding of localized phenomena was not possible; hence, tests on the recycled elastomer should be performed, and ad-hoc material models should be introduced to describe the nonlinearities of the elastomeric compound undergoing large deformations. Furthermore, the RR-FRBs isolator modelling results showed that the bearing stiffness behavior was represented by 2nd-order analytical laws to fit the numerical results. Due to the excessive computational time, it was not possible to insert the FEA of the bearing into a full-scale structural analysis. Therefore, the non-linear laws were assigned to simple connector elements, which replaced the bearings in large analyses. This modelling technique was applied to a dynamic analysis of a liquid storage isolated tank. All of the analyses showed the expected acceleration reduction and period shift, and the validity of the design choices was documented and verified by modal analyses as well as by displacement and stress checking (Spizzuoco et al., 2014). In the research made in 2013 by Gioacchini et al. the Ogden model was used to analyze a rubber isolator without reinforcement and core confined, proposed for residential and commercials low rise buildings, where the axial load is low. The hyperelastic parameters were obtained simultaneously from tension, compression and shear tests made on rubber specimens. The model was validated for a compression load, presenting good correlations with the force-displacement experiments curves (Gioacchini, Tornello, & Frau, 2013). To determine the best option to represent the tests' results, in 2008 Mordini et al. used and fitted both Neo Hooke and Ogden models for the GFRB. Unlike the RR-FRB, in this case, the material properties were identified through a uniaxial

test performed on a dumbbell specimen. The Ogden model provided a higher stiffness. The effect of the bulk modulus was higher on the vertical stiffness, whereas the effect of the shear modulus was higher on the horizontal stiffness. Hence, there were not significant differences between the two models in the vertical stiffness because the bulk modulus was constant for both (Mordini & Strauss, 2008).

A different constitutive model was used for the FEA of STRP isolators. The Mooney–Rivlin material law was employed, which is well suited for most practical applications involving cord-reinforced rubber material. Similar to the GFRB case, to represent the behavior of STRP isolators accurately, the hyperelastic material constants were derived by uniaxial tension tests of dumbbell specimens. An experimental data fitting technique was used to determine the representative material constants. The finite element model was extremely accurate in simulating the force–displacement relationships of the STRP isolators. Both cases, 80% and 130% maximum lateral displacement with regard to the total rubber thickness, were in close agreement with the experimental tests results. However, for a lower level of lateral displacement, the accuracy of the FEA was reduced (Mishra et al., 2013).

The investigations made in 2010 by Toopchi-Nezhad, in 2014 by Van Engelen et al., in 2014 by Osgooei et al. and in 2015 by Al-Anany and Tait are examples of FEA that can be used to predict an isolator's behavior. Toopchi-Nezhad simulated the lateral responses of a bonded elastomeric isolator (B-FREI) and a stable unbonded isolator (SU-FREI). Both isolators were made from the same materials and geometrical properties and were subjected to identical constant vertical loading. Comparing the lateral responses, it was found that the SU-FREI was considerably more efficient than that of the B-FREI as a seismic isolator. In addition, the in-service stress demands on the SU-FREI were found to be significantly lower than that on the B-FREI (Toopchi-Nezhad, Tait, & Drysdale, 2011). Van Engelen et al. (2015) proposed partially bonded fiber-reinforced elastomeric isolators (PB-FREIs) to allow the transfer of tensile forces and to address concerns over permanent displacement due to slip under certain loading conditions in SU-FREIs. Preliminary experimental and FEA demonstrated that large portions of the isolator could be bonded without notably influencing the rollover characteristics of the isolator. Furthermore, softening was prevented when the bonded portion prohibited further loss of contact and prevented additional rollover. The PB-FREIs retained the beneficial characteristics of SU-FREIs and B-FREIs (Van Engelen et al., 2015). Osgooei et al. (2014) analyzed non-axisymmetric square isolators through a three-dimensional FEA to identify the lateral response characteristics of the bearings when loaded at 15°, 30° and 45°. The results showed that the effective lateral stiffness of the bearings increases as the loading direction changes and as the aspect ratio decreases. According to the results, if the goal is to maintain a constant lateral response behavior under various loading directions, it is recommended that higher aspect ratio values be considered for square, unbonded FREIs (Osgooei et al., 2014). Al-Anany and Tait employed a finite element model to analyze infinitely long strip fiber-reinforced elastomeric isolators under vertical and rotational loadings. The performance of isolators with different aspect ratios under different axial loads and angles of rotation and the resulting stress and strain states were evaluated both with bonded and unbonded boundary conditions. It was concluded that the unbonded conditions resulted in a better behavior and that the isolators with lower aspect ratios have lower normal stresses under combined vertical and rotational loadings and lower vertical and rotational stiffness values (Al-Anany & Tait, 2015).

5. RESULTS OVERVIEW

In Table 1 and Figures 1 to 3, the results obtained in each of the aforementioned studies are shown and they are enumerated according to the order of appearance in the reference list. Several mechanical properties were calculated by the authors taking into account these results and the equations $K_v = E_c A/t_r$ and $K_h = GA/t_r$,; where K_v is the vertical stiffness of the rubber bearing, K_h is the horizontal stiffness, A is the loaded area of the bearing, t_r is the total thickness of rubber in the bearing, E_c is the instantaneous compression modulus of the composite under the specified level of vertical load, and G is the shear modulus of the rubber (Kelly & Konstantinidis, 2011).

From Table 1 and Figures 1 to 3, was observed that, although circular devices are commonly used on constructions, square and rectangular shapes were selected for the mentioned research purposes. This provides the option of analyzing the devices under horizontal loads

applied in different directions and gives the possibility to use them on buildings with a wall structural system, which are common in residential cases. Shape factors less than 10 were used in 42% of the cases despite higher values are suggested to guarantee an adequate vertical stiffness and reduced vertical deformations and amplifications of the accelerations (Naeim & Kelly, 1999). Regarding the matrix material, natural rubber and neoprene were the options selected to manufacture the bearings with high damping values. This reduces the cost of the devices because additional damping enhancement mechanisms could be avoided. Recycled rubber is a convenient alternative also, especially to improve the manufacture process due to the layers are united by using a chemical adhesive eliminating the vulcanization phase. In spite of difference between materials and dimensions of the devices, it was observed that with carbon fiber reinforcement, the best mechanical properties were obtained (vertical and horizontal stiffness, and damping). Finally, taking into account that the matrix in each isolator varies according to its composition (materials and dosing), it is not possible to select one hyperelastic model for all cases when a FEA is made; however, Mooney–Rivlin and Neo-Hookean, which is a derivation of the first one, are the options more frequent in the studied cases. This is probably because the Mooney-Rivlin model requires less computational time and experimental tests to calculate the mechanical properties than other models (Dassault Systèmes Simulia Corp., 2016; González, Álvarez, Moya, & Abreu, 2009). It is worth nothing that when a characterization of the material is made, using tension, shear or compression tests, a best fit with experimental results is performed.

Despite the acceptable behavior of carbon fiber reinforced isolators reported in the literature, their actual implementation has been scarce, possibly due to the fact that they are expensive and, in the case of developing countries, that it is necessary to import the fiber. In accordance with Table 1 and Figures 1 to 3, the main disadvantage of using other materials, such as nylon and polyester, is their characteristics in the vertical direction. However, if tensile modulus and thickness were to be increased (Konstantinidis & Kelly, 2014), the prototypes could achieve a vertical stiffness on the same order of magnitude as that of carbon fiber isolators, at a cost up to five time less expensive. Furthermore, in order to obtain a complete knowledge of these devices, a study of the rollover phenomenon should be done, which includes the influence of the vertical characteristics in the horizontal direction, such as the starting point of detachment and the percentage of lost contact area according to displacement levels. Regarding the modelling process, considering that the rubber is hypereslastic and viscous, the FEA models should include both behaviors (e.g. by using Prony series for viscous behavior) and not just hyperleastic behavior as the majority of the previous studies have done. In this way, a better understanding of the isolators could be obtained, allowing buildings to be designed under real operating conditions of the system. This could improve results and lead to cost reductions, which in turn could lead to FREIs being used massively in earthquake prone countries.

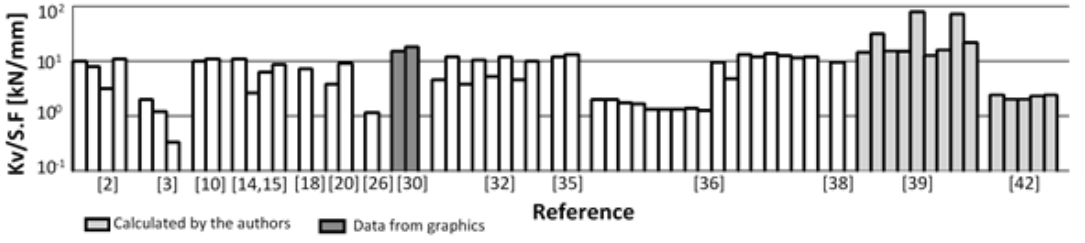

Fig. 1. Ratio Vertical stiffness (Kv) / Shape factor ($S.F$) vs. Isolators researched.

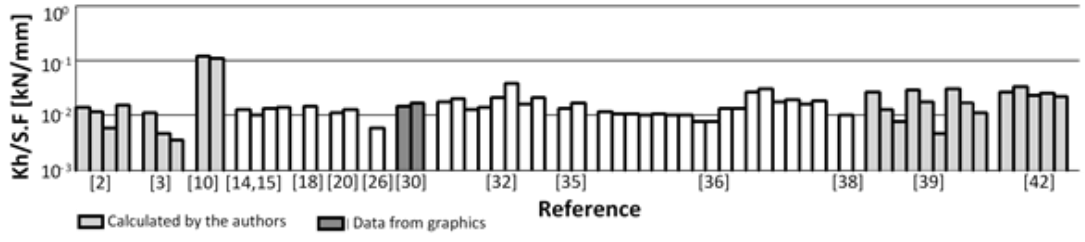

Fig. 2. Ratio Horizontal stiffness (Kh) / Shape factor ($S.F$) vs. Isolators researched.

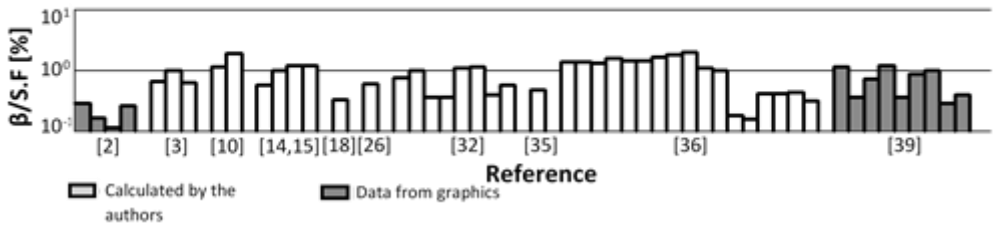

Fig. 3. Ratio Damping (β) / Shape factor (*S.F*) vs. Isolators researched.

Reference	Shape	Size [mm]	Shape Factor	Matrix	Reinforcement	Vertical Properties		Horizontal Properties			Hyperelastic model
						Ec [MPa]	Kv [kN/mm]	G [MPa]	Kh [kN/mm]	β (%)	
[2]	Sq	150x64,85	14.5	R	C -0/90 ,+45/−45	307.7	155.90	0.65	0.35	7.2	
	Sq	150x65,55	22.4	R	C -0/90 ,+45/−45	386.8	202.31	0.68	0.38	6.7	
	Sq	150x75,40	39.8	R	C -0/90 ,+45/−45	451.0	214.07	0.66	0.34	6.0	
	Sq	150x78,30	13.8	R	S	389.6	187.67	0.73	0.38	6.5	
[3]	Ci	150x120	9.4	R	S	176.0	34.29	0.54	0.14	7.8	
	Ci	150x120	9.5	R	C	111.0	15.48	0.40	0.07	9.5	
	Ci	150x120	12.6	R	Pl	35.0	6.53	0.35	0.09	10.3	
[10]	Sq	200x75	4.1	R-HiDa	S	102.9	40.60	0.92	0.75	5.9	Polynomial
	Ci	150x100	3.6	R-HiDa	S	105.3	45.40	1.35	0.49	12.5	
[14, 15]	Sq	70x26,5	11.7	R-HiDa	C-bd	360.0	147.00	0.59	0.24	9.0	Mooney–Rivlin
	Sq	70x33,5	11.7	R-HiDa	C-bd	207.7	56.50	0.47	0.13	12.7	
	Sq	70x36,7	5.8	R-HiDa	C-bd	203.2	47.40	0.56	0.13	9.2	
	Sq	70x38,2	5.8	R-HiDa	C-bd	233.3	54.40	0.58	0.14	9.6	
[17]	Re	200x300x60		R	C		1341.84		3.51	8.1	
	Re	200x300x60		R-H32	C		136.54		3.34	10.4	
	Re	200x300x60		R-LP32	C		1193.55		2.80	12.8	
[17, 18]	Ci	174,5x128	11.0	R-H43	S	256.4	96.00	0.76	0.29	6.2	
	Ci	174,5x128		R-H43	Ny	18.6	35.50	0.14	0.26	11.2	
	Ci	698x345		R-H172	S		1073.22		3.50	6.2	
	Ci	698x345		R-H172	C		3208.57		3.30	15.9	

Calculated by the authors Data from graphics

Nomenclature

Properties G: shear modulus Kv: vertical stiffness Kh: horizontal stiffness Ec: compression modulus β: viscous damping

Shape Sq: square Re: rectangular Ci: circular B: bonded U: unbonded

Size Sq: side x thickness Re: side x side x thickness Ci: diameter x thickness

Matrix R: rubber N: neoprene Na: natural Nn: nanocomposite T: from tire HiDa: high damping LoDa: low damping A: aged H: hole diameter CI: cut interior CE: cut exterior LP: lead plug diameter GY: Goodyear tire M: Michelin tire Pi: Pirelli tire La: Lassa tire

Reinforcement S: steel plate Ny: nylon fiber C: carbon fiber Pt: polyester G: glass Ep: engineering plastic Pm: plastic mesh Pl: polyamide F-01: fiber FIBP-01 qd: quadri-directional bd: bidi-directional 0/90: fiber orientation +45/-45: fiber orientation

Table. 1. Properties of isolator prototypes and model.

Reference	Shape	Size [mm]	Shape Factor	Matrix	Reinforcement	Vertical Properties		Horizontal Properties			Hyperelastic model
						Ec [MPa]	Kv [kN/mm]	G [MPa]	Kh [kN/mm]	β (%)	
[20]	Sq	150	18.8	R	C -0/90 ,+45/–45	223.0	116.66	0.54	0.28		
	Sq	150	18.8	R-Nn	C -0/90 ,+45/–45	343.2	179.49	0.69	0.36		
[26]	Sq	100x72	15.0	R-T	S-T	152.3	21.13	0.10	0.12	12.0	Mooney–Rivlin
[29]	Re	200x300x43		R	Pt		175.00	0.72			
	Re	200x300x43		R	Ny		595.00	0.72			
	Re	200x300x43		R	F-01		135.00	1.26			
	Re	200x300x43		R	F-05		150.00				
	Re	200x300x43		R	C		325.00				
	Re	200x300x43		R	G		152.78				
[30]	Sq	490x150	20.4	R	G-bd	1265.8	511.11	0.45	0.54		Neo Hookean
	Sq	490x150	20.4	R	G-bd	1265.8	663.16	0.45	0.63		Ogden
[32]	Ci	150x69,4	8.75	R-Na	C-bd,Pm	164.8	60.66	0.77	0.29	7.7	
	Ci	150x79	8.75	R-Na	S	386.0	142.10	0.89	0.33	9.0	
	Ci	150x62,4	17.5	R-Na	C-bd,Pm	242.6	107.18	0.73	0.32	10.3	
	Ci	150x79	17.5	R-Na	S	474.4	209.57	0.95	0.42	10.5	
	Ci	150x69,4	8.75	R-Na,LP30	C-bd,Pm	177.8	65.47	0.94	0.35	11.6	
	Ci	150x79	8.75	R-Na,LP30	S	377.0	138.81	1.46	0.54	13.2	
	Ci	150x62,4	17.5	R-Na,LP30	C-bd,Pm	276.1	121.99	1.12	0.49	11.2	
	Ci	150x79	17.5	R-Na,LP30	S	423.3	187.01	1.61	0.71	13.7	
[35]	Sq	240x111	12.0	R	Ep	196.4	205.66	0.39	0.27	8.6	
	Sq	240x111	12.0	R	S	232.4	243.36	0.39	0.36		

Calculated by the authors Data from graphics

Nomenclature

Properties G: shear modulus Kv: vertical stiffness Kh: horizontal stiffness Ec: compression modulus β: viscous damping

Shape Sq: square Re: rectangular Ci: circular B: bonded U: unbonded

Size Sq: side x thickness Re: side x side x thickness Ci: diameter x thickness

Matrix R: rubber N: neoprene Na: natural Nn: nanocomposite T: from tire HiDa: high damping LoDa: low damping A: aged H: hole diameter CI: cut interior CE: cut exterior LP: lead plug diameter GY: Goodyear tire M: Michelin tire Pi: Pirelli tire La: Lassa tire

Reinforcement S: steel plate Ny: nylon fiber C: carbon fiber Pt: polyester G: glass Ep: engineering plastic Pm: plastic mesh Pl: polyamide F-01: fiber FIBP-01 qd: quadri-directional bd: bidi-directional 0/90: fiber orientation +45/-45: fiber orientation

Table. 1. Properties of isolator prototypes and model - Continuation.

Table. 1. Properties of isolator prototypes and model - Continuation.

Reference	Shape	Size [mm]	Shape Factor	Matrix	Reinforcement	Vertical Properties		Horizontal Properties			Hyperelastic model
						Ec [MPa]	Kv [kN/mm]	G [MPa]	Kh [kN/mm]	β (%)	
[36]	Sq	90x43,68	8.0	N	C-bd	150.8	29.08	0.90	0.13	16.9	
	Sq	85x41,99	8.5	N	C-bd	170.7	30.84	0.90	0.11	18.9	
	Sq	82x41,99	8.2	N	C-bd	154.4	25.96	0.90	0.10	16.6	
	Sq	79x41,99	7.9	N	C-bd	147.3	22.98	0.90	0.08	21.7	
	Sq	77,5x41,99	7.8	N	C-bd	103.2	15.50	0.90	0.09	19.2	
	Sq	76x41,99	7.6	N	C-bd	111.6	16.11	0.90	0.08	18.5	
	Sq	74,5x41,99	7.5	N	C-bd	113.2	15.71	0.90	0.07	22.1	
	Sq	73x41,99	7.3	N	C-bd	124.0	16.52	0.90	0.07	24.4	
	Sq	71x41,99	7.1	N	C-bd	100.5	12.66	0.90	0.06	25.7	
	Sq	120x51,18	10.0	N	C-qd	327.8	98.33	0.90	0.21	12.4	
	Sq	120x51,18	10.0	N	C-qd	236.5	70.94	0.90	0.22	10.6	
	Sq	240x52,02	23.0	N-LoDa	C-bd	397.6	458.02	1.15	1.11	7.5	
	Sq	240x52,02	23.0	N-LoDa,A	C-bd	324.7	374.08	1.15	1.25	6.5	
	Sq	240x54,03	23.0	R-HiDa,Na	C-qd	449.6	517.89	0.80	0.73	15.1	
	Sq	240x54,03	23.0	R-HiDa,Na,A	C-qd	372.1	428.66	0.80	0.83	15.0	
	Sq	240x52,02	23.0	R-HiDa,Na	C-bd	314.2	361.91	0.80	0.67	15.4	
	Sq	240x52,02	23.0	R-HiDa,Na,A	C-bd	329.0	378.99	0.80	0.79	12.3	
[38]	Sq	70x63	3.5	R-T	C-qd	415.9	33.97	0.49	0.04		Neo-Hookean

Calculated by the authors Data from graphics

Nomenclature

Properties G: shear modulus Kv: vertical stiffness Kh: horizontal stiffness Ec: compression modulus β: viscous damping

Shape Sq: square Re: rectangular Ci: circular B: bonded U: unbonded

Size Sq: side x thickness Re: side x side x thickness Ci: diameter x thickness

Matrix R: rubber N: neoprene Na: natural Nn: nanocomposite T: from tire HiDa: high damping LoDa: low damping A: aged H: hole diameter CI: cut interior CE: cut exterior LP: lead plug diameter GY: Goodyear tire M: Michelin tire Pi: Pirelli tire La: Lassa tire

Reinforcement S: steel plate Ny: nylon fiber C: carbon fiber Pt: polyester G: glass Ep: engineering plastic Pm: plastic mesh Pl: polyamide F-01: fiber FIBP-01 qd: quadri-directional bd: bidi-directional 0/90: fiber orientation +45/-45: fiber orientation

Reference	Shape	Size [mm]	Shape Factor	Matrix	Reinforcement	Vertical Properties		Horizontal Properties			Hyperelastic model
						Ec [MPa]	Kv [kN/mm]	G [MPa]	Kh [kN/mm]	β (%)	
[39]	Sq-B	180x44,6	8.7	R-Na	C-bd	275.2	214.83	0.55	0.43	12.2	
	Sq-B	180x45	20.5	R-Na	C-bd	1326.4	1124.97	0.47	0.40	12.2	
	Sq-B	180x71	20.5	R-Na	C-bd	973.6	524.00	0.35	0.19	17.5	
	Sq-U	180x74,6	8.7	R-Na	C-bd	292.8	228.63	0.58	0.45	14.4	
	Sq-U	180x75	20.5	R-Na	C-bd	2201.2	1866.97	0.78	0.66	12.2	
	Sq-U	180x101	20.5	R-Na	C-bd	705.5	379.71	0.25	0.13	19.2	
	Sq-B	180x79,4	8.7	R-Na	S	302.9	236.51	0.60	0.47	9.0	
	Sq-B	180x85,2	20.5	R-Na	S	2088.3	1771.23	0.74	0.63	10.5	
	Sq-B	180x117,2	20.5	R-Na	S	1552.1	835.36	0.55	0.30	12.9	
[41]	Sq	150x40		R	S	25					
	Re	200x180x46		R-T,GY	S-T	95		0.70	0.56	19.0	
	Re	200x180x69		R-T,GY	S-T	94					
	Re	200x190x46		R-T,Mi	S-T	181					
	Re	200x175x40		R-T,Pi	S-T	74		1.00	0.93	18.0	
	Re	200x180x50		R-T,La	S-T	124		1.10	0.80	19.5	
[42]	Re	76x52x22,35	4.9	N		101.3	21.00	0.70	0.15		James-Green-Simpson Neo-Hookean
	Re	76x52x22,35	3.3	N-H24,CI	C-bd	67.0	12.31	1.03	0.19		
	Re	76x52x22,35	3.7	N-H18,CI	C-bd	69.0	13.39	0.84	0.16		
	Re	76x52x22,35	3.9	N-H24,CE	C-bd	91.0	16.72	1.00	0.18		
	Re	76x52x22,35	4.2	N-H18,CE	C-bd	93.0	18.05	0.88	0.17		

Calculated by the authors Data from graphics

Nomenclature

Properties G: shear modulus Kv: vertical stiffness Kh: horizontal stiffness Ec: compression modulus β: viscous damping

Shape Sq: square Re: rectangular Ci: circular B: bonded U: unbonded

Size Sq: side x thickness Re: side x side x thickness Ci: diameter x thickness

Matrix R: rubber N: neoprene Na: natural Nn: nanocomposite T: from tire HiDa: high damping LoDa: low damping A: aged H: hole diameter
CI: cut interior CE: cut exterior LP: lead plug diameter GY: Goodyear tire M: Michelin tire Pi: Pirelli tire La: Lassa tire

Reinforcement S: steel plate Ny: nylon fiber C: carbon fiber Pt: polyester G: glass Ep: engineering plastic Pm: plastic mesh Pl: polyamide
F-01: fiber FIBP-01 qd: quadri-directional bd: bidi-directional 0/90: fiber orientation +45/-45: fiber orientation

Table. 1. Properties of isolator prototypes and model - Continuation.

6. CONCLUSIONS

The organization and presentation of the results allows to identify important aspects implemented in different experimental programs and analytical models developed for low-cost isolators. This includes the information about the types of materials and dimensions used, as well as the mechanical properties obtained.

Fiber-reinforced isolators or scrap tire rubber pad isolators are shown as an adequate option to be used for seismic isolation of structures, particularly for ordinary low-rise residential and commercial buildings, due to their lighter weight and simpler manufacturing process compared with that of steel-reinforced elastomeric isolators.

Options for the matrix included external (cuts and holes) and internal modifications (nanocomposite) using natural rubber or neoprene, as well as recycled rubber from tires or industrial leftover. For a conventional fiber reinforcement, the experimental results show that the behavior of carbon fiber is better than that of glass and nylon fiber, especially when is used in quadri-directional fabrics. Furthermore, non-conventional fibers, like carbon-fiber-reinforced plastics mesh and an engineering plastic sheet, are presented as good alternatives to be implemented on isolators.

Finite element analyses using constitutive models, such as the Polynomial, Monney–Rivlin, Neo-Hooke or Ogden models, agree extremely well with the experimental results. Nevertheless, tests on the base material should be performed to identify the nonlinearities of the elastomer.

CONFLICT OF INTEREST

The authors have no conflicts of interest to declare.

REFERENCES

Al-Anany, Y. M., & Tait, M. J. (2015). A numerical study on the compressive and rotational behaviour of fiber reinforced elastomeric isolators (FREI). *Composite Structures, 133*, 1249–1266.

Ashkezari, G. D., Aghakouchaka, A. A., & Kokabib, M. (2008). Design, manufacturing and evaluation of the performance of steel like fiber reinforced elastomeric seismic isolators. *Journal of materials processing technology, 197*, 140–150.

Bakhshi, A., Jafari, M. H., & Tabrizi, V. V. (2014). Study on dynamic and mechanical characteristics of carbon fiber- and polyamide fiber-reinforced seismic isolators. *Materials and Structures, 47*, 447–457.

Buckle, I. G. (2000). Passive control of structures for seismic loads. *Bulletin of the New Zealand Society for Earthquake Engineering, 12WCEE 2000*.

Cardone, Donatello, Gesualdi, G., & Nigro, D. (2011). Effects of air temperature on the cyclic behavior of elastomeric seismic isolators. *Bull Earthquake Eng., 9*, 1227–1255.

Casciati, F., & Faravelli, L. (2012). Experimental investigation on the aging of the base isolator elastomeric component. *Acta Mech, 223*, 1633–1643.

Dassault Systèmes Simulia Corp. (2016, 06 20). *Abaqus 6.10 Documentation*. Retrieved from http://abaqusdoc.ucalgary.ca/books/usb/default.htm?startat=pt05ch19s05abm07.html#usb-mat-chyperelastic

Gent, A. N. (2012). *Engineering with Rubber*. Cincinnati: Hanser Publications.

Gioacchini, G., Tornello, M. E., & Frau, C. D. (2013). Validación de un modelo numérico para un nuevo dispositivo de aislamiento sísmico. *Mecánica Computacional, 32*, 793-805.

Gjorgjiev, I., & Garevski, M. (2013). A polynomial analytical model of rubber bearings based on series of tests. *Engineering Structures, 56*, 600–609.

Gómez, D. (2008). Sistemas de control para la protección de estructuras civiles sometidas a cargas dinamicas.*Dyna*, 77-89.

González, R., Álvarez, E., Moya, J. L., & Abreu, K. (2009). Modelos de materiales hiperelásticos para el análisis de los elastómeros usando el MEF. *Ingeniería Mecánica, 12*, 57-66.

Hallad, S. A., Banapurmatha, N. R., Hunashyala, A. M., Shettara, A. S., Ayachitd, N. H., A.K., M., . . . Uttur, M. (2017). Original Experimental investigation for graphene and carbon fibre in polymer-basedmatrix for structural applications. *Journal of Applied Research and Technology*, 297-302.

Hedayati, F., & Shahria, M. (2014a). Sensitivity analysis of carbon fiber-reinforced elastomeric isolators based on experimental tests and finite element simulations. *Bulletin Earthquake Engineering, 12*, 1025-1043.

Hedayati, F., & Shahria, M. (2014b). Performance of carbon fiber-reinforced elastomeric isolators manufactured in a simplified process: experimental investigations. *Structural Control and Health Monitoring, 21*, 1347–1359.

Ibrahim, R. (2008). Recent advances in nonlinear passive vibration isolators. *Journal of Sound and Vibration, 314*, 371-452.

Kang, B.-S., Kang, G.-J., & Moon, B.-Y. (2003). Hole and lead plug effect on fiber reinforced elastomeric. *Journal of Materials Processing Technology, 140*, 592–597.

Kang, G. J., & Kang, B. S. (2009). Dynamic analysis of fiber-reinforced elastomeric isolation structures. *Journal of Mechanical Science and Technology, 23*, 1132-1141.

Kelly, J. M., & Konstantinidis, D. A. (2011). *Mechanics of rubber bearings for seismic and vibration isolation.* California: Wiley.

Khanlari, S., Dehghani, G., Kokabi, M., & Razzaghi, M. (2010). Fiber-Reinforced nanocomposite seismic isolators: design and manufacturing. *Polymer Composites*, 299-306.

Konstantinidis, D., & Kelly, J. M. (2014). Advances in Low-Cost Seismic Isolation with Rubber. *Tenth U.S. National Conference on Earthquake Engineering Frontiers of Earthquake Engineering, 10NCEE.*

Ledezma-Ramirez, D. F., Ferguson, N., & Brennan, M. (2010). Shock Performance of Different Semiactive Damping Strategies. *Journal of Applied Research and Technology*, 249-259.

Martelli, A., & Forni, M. (2010). Seismic isolation and other anti-seismic sytems recent applications in Italy and worldwide. *Seismic Isolation and Protection Systems, 1*, 75-123.

Melkumyan, M. G. (2013). Comparison of the analyses results of seismic isolated buildings by the design code and Time Histories. *Journal of Civil Engineering and Science, 2*,184-192.

Melkumyan, M. G., Loo, S., Fuller, K. N., Vardanian, G. K., Bejbutian, L. B., Nersessian, T. E., . . . Kazarianazarian, V. A. (2000). Testing of a full scale base isolated four story apartment. *12th World Conference on Earthquake Engineering, 12WCEE2000.*

Mishra, H. K., Igarashi, A., & Matsushima, H. (2013). Finite element analysis and experimental verification of the scrap tire rubber pad isolator. *Bulletin of Earthquake Engineering, 11*, 687–707.

Mkrtycheva, O., Dzhinchvelashvilia, G., & Bunov, A. (2014). Study of lead rubber bearings operation with varying height buildings at earthquake. *Procedia Engineering, 91*, 48-53.

Moon, B. Y., Kang, G. J., Kang, B. S., Kim, G. S., & Kelly, J. M. (2003). Mechanical properties of seismic isolation system with fiber-reinforced bearing of strip type. *International Applied Mechanics, 39*, 133-142.

Moon, B.-Y., Kang, G.-J., Kang, B.-S., & Kelly, J. M. (2002). Design and manufacturing of fiber reinforced elastomeric isolator for seismic isolation. *Journal of Materials Processing Technology, 130-131*, 145-150.

Mordini, A., & Strauss, A. (2008). An innovative earthquake isolation system using fibre reinforced rubber bearings. *Engineering Structures, 30*, 2739–2751.

Naeim, F., & Kelly, J. M. (1999). *Design of seismic isolated structures from theory to practice.* New York: John Wiley & Sons, Inc.

Naghshineh, A. K., Akyüz, U., & Caner, A. (2014). Comparison of fundamental properties of new types of fiber-mesh reinforced seismic isolators with conventional isolators. *Earthquake Engineering & Structural Dynamics, 43*, 301-316.

Osgooei, P. M., Tait, M. J., & Konstantinidis, D. (2014). Finite element analysis of unbonded square fiber-reinforced elastomeric isolators (FREIs) under lateral loading in different directions. *Composite Structures, 113*, 164–173.

Osgooei, P. M., Van Engelen, N. C., Konstantinidis, D., & Tait, M. J. (2015). Experimental and finite element study on the lateral response of modified rectangular fiber-reinforced elastomeric isolators (MR-FREIs). *Engineering Structures, 85*, 293–303.

Ping, T., Kai, X., Bin, W., ChiaMing, C., Han, L., & FuLin, Z. (2014). Development and performance evaluation of an innovative low-cost seismic isolator. *Science China Technological Sciences, 57*, 2050-2061.

Russo, G., Pauletta, M., & Cortesia, A. (2013). A study on experimental shear behavior of fiber-reinforced elastomeric isolators with various fiber layouts, elastomers and aging conditions. *Engineering Structures, 52*, 422–433.

Saiful Islam, A., Rizwan Hussain, R., Jameel, M., & Zamin Jumaat, M. (2012). Non-linear time domain analysis of base isolated multi-storey building under site specific bi-directional seismic loading. *Automation in Construction, 22*, 554-566.

Spizzuoco, M., Calabrese, A., & Serino, G. (2014). Innovative low-cost recycled rubber–fiber reinforced isolator: experimental tests and finite element analyses. *Engineering Structures, 76*, 99–111.

Strauss, A., Apostolidi, E., Zimmermann, T., Gerhaher, U., & Dritsos, S. (2014). Experimental investigations of fiber and steel reinforced elastomeric bearings: shear modulus and damping coefficient. *Engineering Structures, 75*, 402–413.

Toopchi-Nezhad, H., Tait, M. J., & Drysdale, R. G. (2011). Bonded vs.unbonded strip fiber reinforced elastomeric isolators: Finite element analysis.*Composite Structures,93*, 850–859.

Turer, A., & Özden, B. (2008). Seismic base isolation using low-cost Scrap Tire Pads (STP). *Materials and Structures, 41*, 891–908.

Van Engelen, N. C., Osgooe, P. M., Tait, M. J., & Konstantinidis, D. (2014). Experimental and finite element study on the compression properties of Modified Rectangular Fiber-Reinforced Elastomeric Isolators (MR-FREIs). *Engineering Structures, 74*, 52-64.

Van Engelen, N., Osgooei, P. M., Tait, M. J., & Konstantinidis, D. (2015). Partially bonded fiber-reinforced elastomeric isolators (PB-FREIs). *Structural Control and Health Monitoring, 22*, 417-432.

Vidal-Lesso, A., Ledesma Orozco, E., Lesso Arroyo, R., & Rodríguez Castro, R. (2011). Dynamic Response of Femoral Cartilage in Knees with Unicompartmental Osteoarthritis. *Journal of Applied Research and Technology, 9*, 173-187.